J|A|C|S
ARTICLES
Published on Web 07/09/2004

Assembling of Amphiphilic Highly Branched Molecules in Supramolecular Nanofibers

Maryna Ornatska, Sergiy Peleshanko, Kirsten L. Genson, Beth Rybak, Kathy N. Bergman, and Vladimir V. Tsukruk*

Contribution from the Materials Science and Engineering Department, Iowa State University, Ames, Iowa 50011

Received January 7, 2004; E-mail: vladimir@iastate.edu

Abstract: We found that the amplification of weak multiple interactions between numerous peripheral branches of irregular, flexible, polydisperse, and highly branched molecules can facilitate their self-assembly into nanofibrillar micellar structures at solid surfaces and the formation of perfect long microfibers in the course of crystallization from solution. The core−shell architecture of the amphiphilic dendritic molecules provides exceptional stability of one-dimensional nanofibrillar structures. The critical condition for the formation of the nanofibrillar structures is the presence of both alkyl tails in the outer shell and amine groups in the core/inner shell. The multiple intermolecular hydrogen bonding and polar interactions between flexible cores stabilize these nanofibers and make them *robust albeit flexible*. This example demonstrates that one-dimensional supramolecular assembling at different spatial scales (both nanofibers and microfibers) can be achieved without a tedious, multistep synthesis of shape-persistent molecules.

Introduction

Dendritic molecules are long thought as a promising building block for the interfacial organic assemblies for organized templates and surface nanostructures with tunable properties.[1−3] The variation of hydrophobic and hydrophilic interactions by changing the composition of terminal branches and cores of these treelike molecules is considered to be a powerful tool for inducing organized supramolecular structures at surfaces and interfaces.[1,4−9] Because of architectural symmetry, a vast majority of dendritic molecules studied to date possess globular or near globular shapes in solution, in bulk, and at weakly interacting interfaces.[1,2,5,10,11] Only specially designed dendritic molecules with peculiar architectures usually related to sterically asymmetric fragments were shown to be capable of forming self-assembled one-dimensional supramolecular structures such as rods, fibers, ribbons, and helices, all shapes with a special interest for nanotechnology. The chemical architectures successfully used for these arrangements included shape-persistent planar dendrimers, hairy rod and discotic polymers, rod-coils, and tapered molecules.[1,2,12−14] A proper combination of steric constraints, stacking interactions, internal rigidity, and hydrogen bonding is postulated to be critical for precise assembly of these shape-persistent molecules into large-scale, uniform, one-dimensional supramolecular structures in solution, in bulk state, and at interfaces.

The self-organization of long (several centimeters) fibers via noncovalent synthesis of low molar weight compounds composed of various amphiphiles from amino derivatives, with fluorinated chains, and phospholipids was reported.[15,16] Stupp et al. developed a synthetic strategy that included different combinations of rod segments with precisely placed functional groups and a variety of branched terminations to assemble organized structures via balanced steric and intermolecular interactions (rod-dendron molecules).[17] The variation of the chemical composition, the symmetry of molecules, and the generation of the dendron blocks resulted in the formation of cubic, lamellar, and cylindrical microstructures in the bulk state with occasional assembly in long, uniform one-dimensional ribbons and fibers. It is widely accepted that a precise "match-

(1) *Dendrimers and Other Dendritic Polymers*; Frechet, J. M. J., Tomalia, D. A., Eds.; Wiley & Sons: London, 2002.
(2) (a) Sheiko, S. S.; Moller, M. *Chem. Rev.* **2001**, *101*, 4099. (b) Percec, V.; Cho, W. D.; Ungar, G. *J. Am. Chem. Soc.* **2000**, *122*, 10273.
(3) (a) Tsukruk, V. V. *Prog. Polym. Sci.* **1997**, *22*, 247. (b) Tsukruk, V. V. *Adv. Mater.* **2001**, *13*, 95. (c) Luzinov I.; Minko, S.; Tsukruk, V. V. *Prog. Polym. Sci.* **2004**, *29*, 635.
(4) (a) Brunsveld, L.; Folmer, J.; Meijer, E. W.; Sibesma, R. *Chem. Rev.* **2001**, *101*, 4071. (b) Zeng, F.; Zimmerman, S. C. *Chem. Rev.* **1997**, *97*, 1681.
(5) Tsukruk, V. V.; Rinderspacher, F.; Bliznyuk, V. N. *Langmuir* **1997**, *13*, 2171.
(6) Weener, J.-W.; Meijer, E. W. *Adv. Mater.* **2000**, *12*, 741.
(7) Jonkheim, P.; Hoeben, F. J.; Kleppinger, R.; van Herrikhuyzen, J.; Schnenning, A. P.; Meijer, E. W. *J. Am. Chem. Soc.* **2003**, *125*, 15941.
(8) Sui, G.; Micic, M.; Huo, Q.; Leblanc, R. M. *Langmuir* **2000**, *16*, 7847.
(9) (a) Lee, M.; Kim, J.-W.; Peleshanko, S.; Larson, K.; Yoo, Y.; Vaknin, D.; Markutsya, S.; Tsukruk, V. V. *J. Am. Chem. Soc.* **2002**, *124*, 9121. (b) Tsukruk, V. V.; Luzinov, I.; Larson, K.; Li, S.; McGrath, D. V. *J. Mater. Sci. Lett.* **2001**, *20*, 873.
(10) Tsukruk, V. V. *Adv. Mater.* **1998**, *10*, 253.
(11) (a) Tsukruk, V. V.; Shulha, H.; Zhai, X. *Appl. Phys. Lett.* **2003**, *82*, 907. (b) Shulha, H.; Zhai, X.; Tsukruk, V. V. *Macromolecules* **2003**, *36*, 2825.
(12) (a) Zubarev, E. R.; Pralle, M. U.; Sone, E. D.; Stupp, S. I. *J. Am. Chem. Soc.* **2001**, *123*, 4105. (b) Zubarev, E. R.; Pralle, M. U.; Li, L. M.; Stupp, S. I. *Science* **1999**, *283*, 523. (c) Won, Y. Y.; Davis, H. T.; Bates, F. S. *Science* **1999**, *283*, 960. (d) Djalali, R.; Li, S.-Y.; Schmidt, M. *Macromolecules* **2002**, *35*, 4282.
(13) Loi, S.; Butt, H.; Wiesler, U.; Mullen, K. *Chem. Commun*. **2000**, *13*, 1169.
(14) Liu, D.; Zhang, H.; Grim, P. C.; De Feyter, S.; Wiesler, U.; Berresheim, A.; Muellen, K.; De Schryver, F. C. *Langmuir* **2002**, *18*, 2385.
(15) Furhhop, J. H.; Helfrich, W. *Chem. Rev.* **1993**, *93*, 1565.
(16) Menger, M.; Lee, S.; Tao, X. *Adv. Mater.* **1995**, *7*, 669.
(17) (a) Pralle, M. U.; Whitaker, C. M.; Braun, P. V.; Stupp, S. I. *Macromolecules* **2000**, *33*, 3550. (b) Lecommandoux, S.; Klok, H. A.; Sayar, M.; Stupp, S. I. *J. Polym. Sci., Part A: Polym. Chem.* **2003**, *41*, 3501.

Scheme 1. General Schematic of the Chemical Modification of the Hyperbranched Core

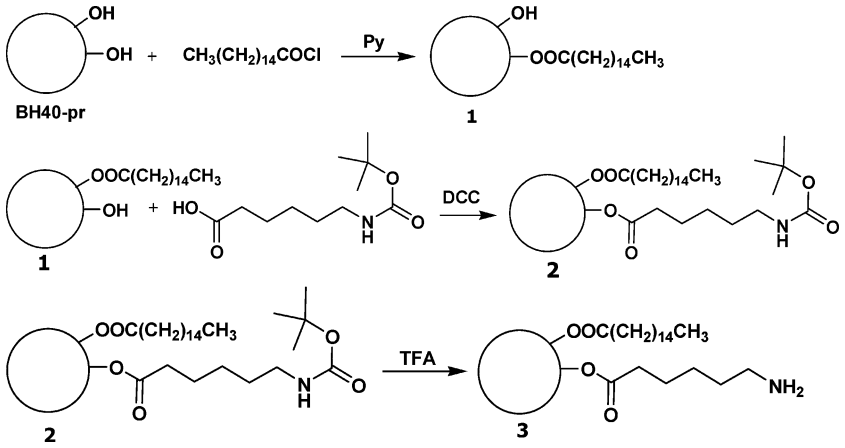

ing" of directional intermolecular interactions and steric constraints is required to facilitate long-range one-dimensional supramolecular assembly of organic and polymeric molecules. From this standpoint, the assembly of organized supramolecular structures from irregular, flexible, dendritic molecules could be very questionable.

Indeed, there are very few reports on the formation of the organized nanostructures from highly branched (hyperbranched) molecules composed of irregular, random branched fragments with the degree of branching well below that observed for ideal dendritic architecture.[18] Because of their irregular architecture, poorly defined shape, and higher polydispersity, they are not expected to form regular supramolecular structures, let alone one-dimensional nanostructures, and are usually considered as good candidates for the applications when no precise structural organization and precisely placed functionalities are required.[19−22]

However, in this report we demonstrate that *multiple weak intermolecular interactions* among *irregular, highly branched, and polydisperse molecules* which are flexible and symmetrical can facilitate their assembly into remarkably well-ordered, one-dimensional supramolecular structures such as long micro- and nanofibers. We suggest that such an unexpected behavior is facilitated by a balance of intermolecular and interfacial interactions caused by appropriate distribution of different functional groups in the outer shell and the inner core of these highly branched molecules. To the best of our knowledge, this is a first example of uniform one-dimensional supramolecular structures assembled from irregular, highly branched molecules.

Results and Discussion

Chemical Modification and Characterization. Highly branched polyester core with hydroxyl terminal groups synthesized by a "one-pot" approach with the presence of active core monomers (so-called hyperbranched molecules of fourth generation) was obtained from Perstorp Polyols and went via the purification and fractionation procedures before further chemical modification (see Supporting Information).[23] The esterification of hyperbranched cores was conducted according to Scheme 1 as suggested in the literature.[24,25]

Final and all intermediate compounds presented in this scheme were completely characterized by FTIR, GPC, ^{1}H NMR, and ^{13}C NMR (see Supporting Information for details). The degree of branching was calculated using integrated intensities of the ^{13}C NMR peaks assigned to different monomeric units, according to the procedure described previously by Hult et al.[26] According to this approach, quaternary carbons of the dendritic, linear, and terminal units can be distinguished by the chemical shifts of 46.91, 48.93, and 50.92 ppm (Figure 1).

The degree of polymerization was estimated from ^{1}H NMR and ^{13}C NMR data as well, according to the procedure suggested by Zagar.[27] This analysis indicated that the chemical composition and the branching structure of the core polyester **BH40-pr** (Scheme 1) were close to the literature data for commercial polyester Boltorn H40.[26,27] According to these calculations the degree of branching of the hyperbranched core after purification was 40%; the average number of monomeric units (the degree of polymerization) was 60, and the number average molecular weight was 7800.

The number of alkyl groups in molecule **3** was determined from ^{13}C NMR spectra using the ratio of the integral intensities of the peaks of the methyl group of the palmitic acid group (14.3 ppm) and methyl group of the poly bis(PMA) (17.8 ppm) (Figure 1). Similarly, the number of boc-6 aminocaproic acid groups (about 14) per molecule **2** was estimated from peaks at 17.8 and 28.6 ppm, assigned to the methyl group of the poly bis(PMA) and to methyl groups of the *tert*-butoxycarbonyl protective group. ^{13}C NMR and ^{1}H NMR spectra of the compound **3** confirm removal of the protective Boc group and exhibit all peaks typical for chemical structures of the core and functional groups (Figure 1). According to this analysis, the amphiphilic molecules **1** and **3** possessed the total molecular weight of 19 200 and 20 800, respectively.

GPC provided additional information about changes in relative molecular weight and the polydispersity of the com-

(18) Frechet, J. M.; Hawker, C. J.; Gitsov, I.; Leon, J. W. *J. Macromol. Sci.* **1996**, *A33*, 1399.
(19) Sunder, A.; Quincy, M.-F.; Mulhaupt, R.; Frey, H. *Angew. Chem., Int. Ed.* **1999**, *38*, 2928.
(20) Voit, B. *J. Polym. Sci., Part A: Polym. Chem.* **2000**, *38*, 2505.
(21) (a) Sidorenko, A.; Zhai, X. W.; Tsukruk, V. V. *Langmuir* **2002**, *18*, 3408. (b) Sidorenko, A.; Zhai, X. W.; Simon, F.; Pleul, D.; Greco, A.; Tsukruk, V. V. *Macromolecules* **2002**, *35*, 5131.
(22) Stiriba, S.-E.; Kautz, H.; Frey, H. *J. Am. Chem. Soc.* **2002**, *124*, 9698.
(23) (a) Mezzenga, R.; Boogh, L.; Manson, J.-A. E.; Pettersson, B. *Macromolecules* **2000**, *33*, 4373. (b) Boogh, L.; Pettersson, B.; Manson, J. A. *Polymer* **1999**, *40*, 2249.
(24) Sunder, A.; Bauer, T.; Muelhaupt, R.; Frey, H. *Macromolecules* **2000**, *33*, 1330.
(25) Holmberg, K.; Hansen, B. *Acta Chem. Scand.* **1979**, *33*, 410.
(26) Claesson, H.; Malmstroem, E.; Johansson, M.; Hult, A. *Acta Polym.* **2002**, *43*, 3511.
(27) Zagar, E.; Zigon, M. *Macromolecules* **2002**, *35*, 9913.

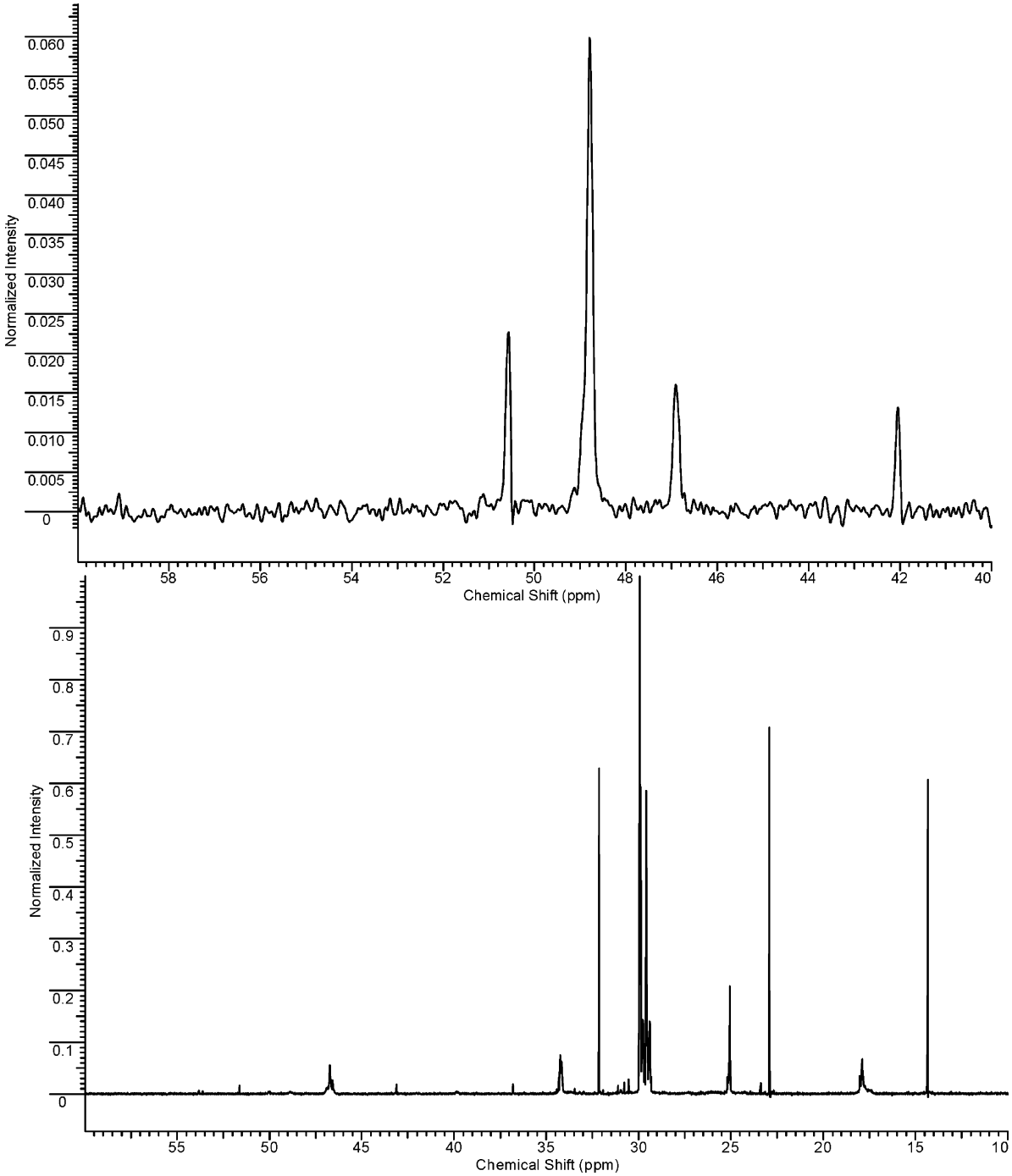

Figure 1. ^{13}C NMR spectra for the fractionated core **BH40-pr** in d_6-DMSO (top) and compound **3** in $CDCl_3$ (bottom).

pounds synthesized (Figure 2). The weight average molecular weight was determined by using polystyrene standards to be 8600 for the fractionated core and increased to 11 500 and 15 600 for molecules **1** and **3**, respectively. These numbers, although represent significant underestimation known for branched molecules, show the same trend as those obtained from NMR data. The polydispersity index (PDI) calculated from GPC data for the initial hyperbranched core after fractionation was 1.52, down from 1.86 from initial commercial product. The PDI remained modest for both modified molecules **1** and **3** studied here: 1.44 and 1.45, respectively.

It is worth noting that these and other numbers as well as the chemical structure presented here should be considered only

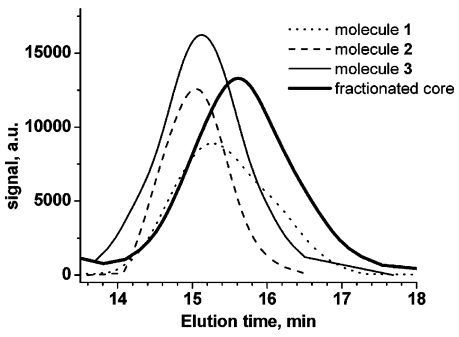

Figure 2. GPC data for final and intermediate compounds.

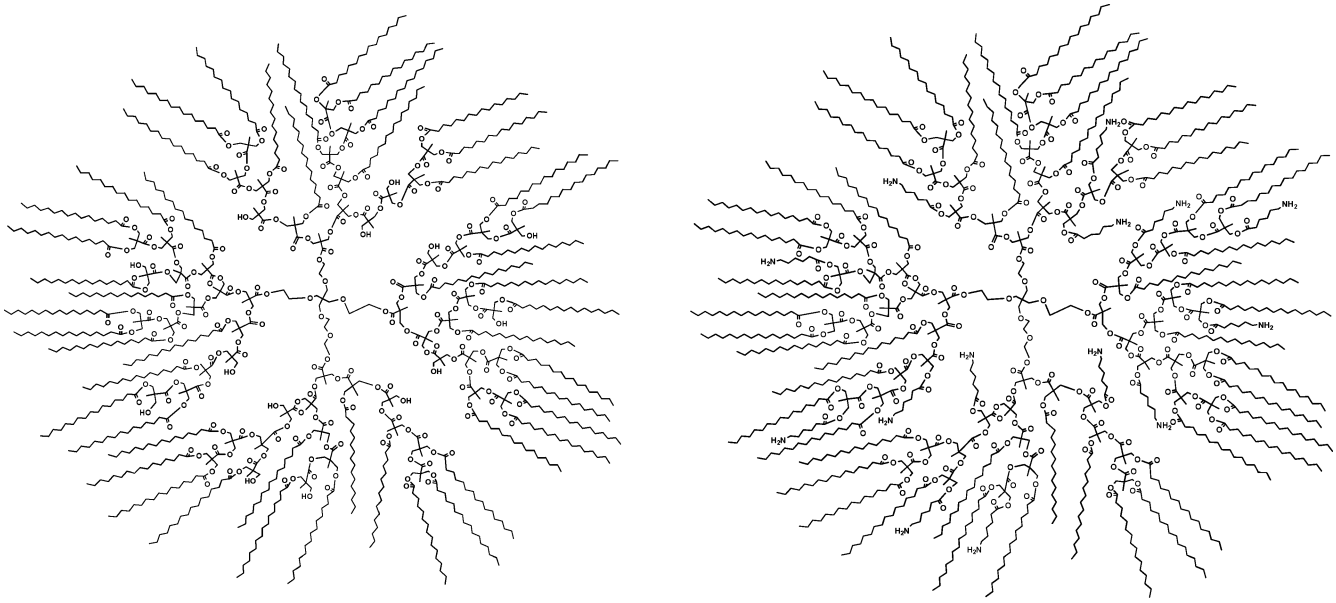

Figure 3. Theoretical chemical structures of the molecules **1** (left) and **3** (right) based on the degree of branching and chemical composition derived from NMR data.

as some average characteristics for irregular hyperbranched architectures as was discussed in numerous publications specifically devoted to this issue.[28−30] For example, it has been demonstrated that the degree of branching is usually within 40−43% for different fractions of the polyester core, but the level of internal cyclization is very low. The number of the terminal hydroxyl groups can be well below the 64 expected for the theoretical model for low molar weight fractions (below 30), but for higher molar weight fraction it is very close to the expected number (64). Theoretical chemical structures of two different amphiphilic hyperbranched molecules with modified shells as determined from the analysis discussed above are presented in Figure 3.

Here, we will focus on two molecules: one molecule with the presence of alkyl tails and hydroxyl and carboxyl groups in the outer shell (molecule **1**) and another molecule combining alkyl tails and residual hydroxyl groups in the outer shell and amine groups in the inner core (molecule **3**) (Scheme 1, Figure 3). The shell of the modified hyperbranched molecules was composed of hydrophobic tails represented by about 50 palmitic (C_{16}) alkyl tails. The inner polyester core contained 15 hydroxyl groups for molecule **1** and about 14 amine- and 1−2 hydroxyl terminated groups for molecule **3**. The amine groups were introduced to enhance polar interactions with silanol surface groups in order to stabilize surface nanostructures transferred on a silicon oxide surface and were proven to be critical for the formation of robust structures.

Surface Behavior. Both amphiphilic hyperbranched molecules at the air−water interface displayed stable monolayers with the surface behavior typical for amphiphilic compounds with well separated and defined polar and hydrophobic fragments (Figure 4). The rising surface pressure observed for the

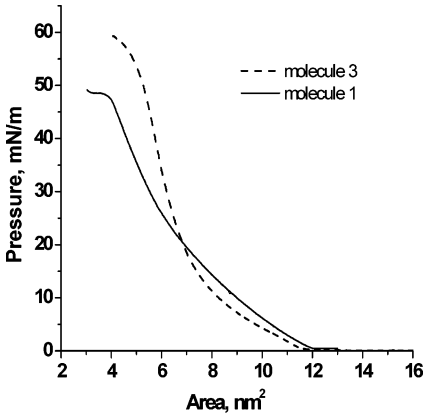

Figure 4. Pressure−area isotherms for molecules.

compression to the area per molecule below 12 nm^2 was fully reversible for both molecules compressed to the pressure in the vicinity of the monolayer collapse (below 35 N/m). This is in sharp contrast to the initial "naked" polyester cores, which desorbed in the water subphase during the compression to the modest surface pressure (see Supporting Information). The rising of the surface pressure during the formation of the condensed Langmuir monolayer is much steeper for molecule **3** indicating that the presence of amine-terminated fragments in the vicinity of the polyester core caused more compact packing of the core−shell structure at the air−water interface with lower compressibility (higher elastic modulus).

Surface Nanostructures. Remarkably, uniform, stable, and consistent one-dimensional surface morphologies were formed by the amphiphilic molecules **3** with amine groups upon transfer onto a silicon surface as can be seen from AFM images obtained in a light tapping mode (Figures 5 and 6).[31] At a low surface pressure (area per molecule within 12−15 nm^2), isolated individual nanofibers were observed. Their overall height of these nanofibers was within 1 nm, and the length was more

(28) (a) Magnusson, H.; Malmstroem, E.; Hult, A. *Macromolecules* **2000**, *33*, 3099. (b) Burgath, A.; Sunder, A.; Frey, H. *Macromol. Chem. Phys.* **2000**, *201*, 782. (c) Hoelter, D.; Burgath, A.; Frey, H. *Acta Polym.* **1997**, *48*, 30.
(29) (a) Chu, F.; Hawker, C. J.; Pomery, P. J.; Hill, D. J. *J. Polym. Sci., Part A: Polym. Chem.* **1997**, *35*, *1627*. (b) Hanselman, R.; Hoelter, D.; Frey, H. *Macromolecules* **1998**, *31*, 3790.
(30) Malmstroem, E.; Johansson, M.; Hult, A. *Macromolecules* **1995**, *28*, 1698.
(31) Ornatska, M.; Peleshanko, S.; Rybak, B.; Holzmueller, J.; Tsukruk, V. V. *Angew. Chem.*, in print

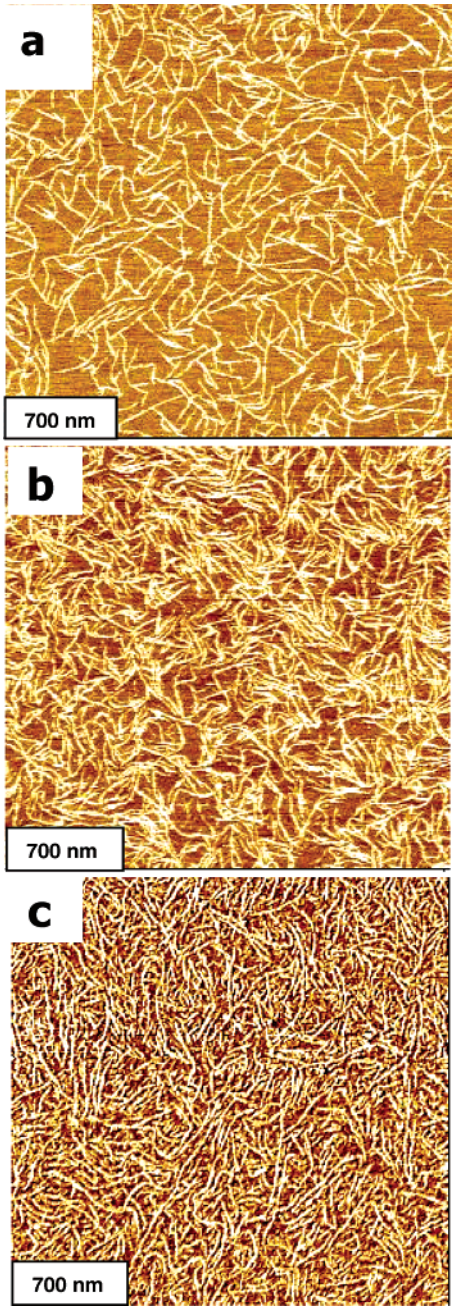

Figure 5. AFM phase images of nanofibrillar structures from molecule **3** at surface pressure: (a) 5 mN/m, (b) 10 mN/m, (c) 20 mN/m.

than 500 nm. The individual nanofibers were modestly curved and possessed a low degree of branching with a frequently observed "punctured" shape (Figure 6). At slightly higher surface pressure, the isolated, very uniform nanofibers were formed all over the surface of the silicon wafers with occasional splitting and sharp bending observed for a small fraction of nanofibers (Figure 5a). At even higher surface pressure, the nanofibers became aggregated in bundles of 3−4 nanofibers demonstrating a local orientational ordering and collective bending (Figure 5b). Finally, at the highest surface pressure, a highly interwoven morphology of densely packed nanofiber with bundles weaving across the large surface areas was observed (Figures 5c and 6a,b). The overall length of these bundles exceeded several microns. The surface area occupied by the nanofibers at higher surface pressures reached 60%, which is close to the "jamming" limit for randomly oriented surface structures.[32] Their interwoven network appeared very similar to a typical texture of nematic liquid crystalline phases with uniform orientational ordering of flexible rodlike molecules and characteristic singularities caused by localized topological defects.[33] The height of these well-defined nanofibrillar structures increased slightly for higher pressures reaching 3−4 nm for densely packed condensed LB monolayers. This was consistent with the effective thickness of the monolayers measured independently from ellipsometry, which indicated the thickness of 3 nm for the highest pressures (see Supporting Information).

High-resolution AFM imaging revealed a widened shape of these nanofibers caused by the usual dilation effect produced by the AFM tip with a typical radius of 10−20 nm (Figure 6). Actual lateral dimensions cannot be determined from these images correctly without deconvolution of the tip shape effect. Considering this, we conducted an independent analysis of the shape of these nanostructures obtained with a very sharp carbon nanotube tip with a calibrated radius (on a gold nanoparticle standard) of curvature below 8 nm. This allowed the direct deconvolution of the tip shape in accordance with the well-known procedures and the estimation of true spatial lateral dimensions of these surface structures. We used both semi-spherical approximation and direct restoration of the tip profile with mathematical morphology approach and observed consistent results.[34] For this analysis, we selected surface areas with well-separated nanostructures and conducted high-resolution scanning with scan sizes not exceeding 600×600 nm^2 (Figure 6c). Then, we ran cross sections perpendicularly to the long axes as demonstrated in Figure 6d and measured both height and apparent lateral dimensions. For example, for three selected nanostructures designated by markers in Figure 6d, we measured the height of 0.8−1 nm and the apparent width of 8.6, 12.3, and 14.1 nm from left to right, respectively. Correction for the tip dilation results in true widths of these features ranging from 5 to 10 nm. The results of this deconvolution analysis conducted for more than 30 individual nanostructures led us to the conclusion that the observed one-dimensional structures were, in fact, *nanofibers* or *nanoribbons* with the lateral dimensions in the range from 4 to 10 nm and heights of 1−4 nm for different surface pressures and surface locations. The lateral dimensions obtained were fairly close to the molecular dimensions estimated from the molecular models in different conformations indicating that these nanofibers are truly molecular fibers composed of individual molecules aggregated in one dimension as will be discussed below.

It is worth noting that these nanofibers preserved their identity (not merging into thicker fibers or into uniform monolayer) even under the highest surface pressure in the vicinity of the monolayer collapse and at the high density of packing. Moreover, the surface structures observed here were exceptionally stable under normal AFM scanning conditions and sustained higher normal forces even in the hard tapping mode. The critical role played by the amine groups attached to the polyester core in the formation of these nanofibrillar structures was supported

(32) Karim, A.; Tsukruk, V. V.; Douglas, J. F.; Satija, S. K.; Fetters, L. J.; Reneker, D. H.; Foster, M. D. *J. Phys. II* **1995**, *5*, 1441.
(33) Tsukruk, V. V.; Shilov, V. V. *Structure of Polymeric Liquid Crystals*; Science: Kiev, 1990.
(34) Tsukruk, V. V.; Gorbunov, V. V. *Probe Microsc.* **2002**, *3*−*4*, 241.

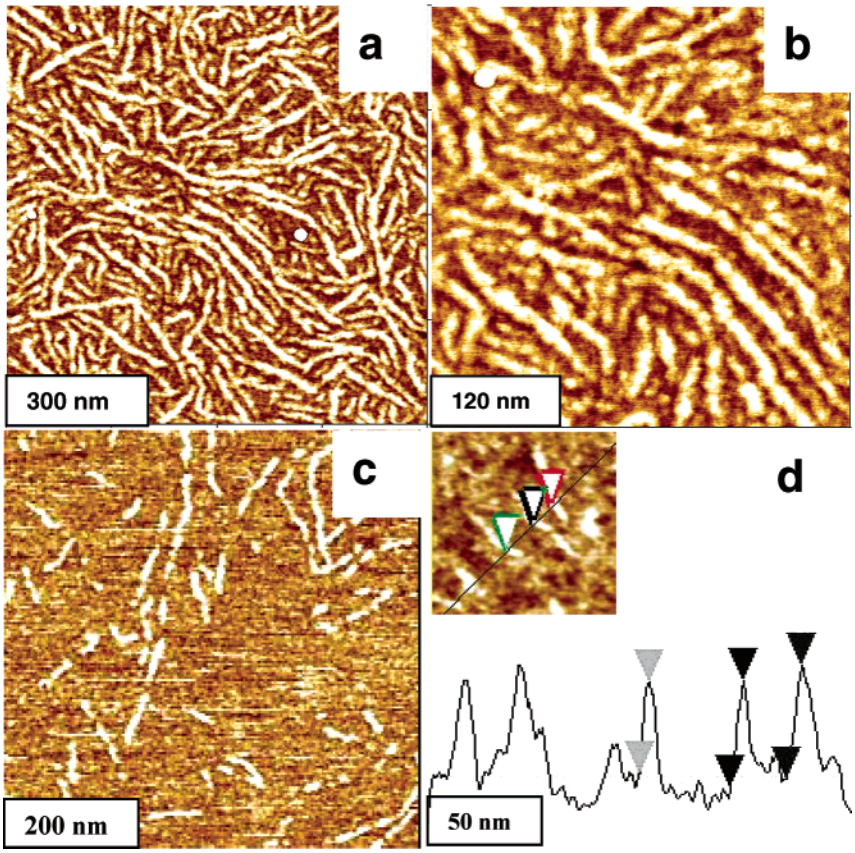

Figure 6. High-resolution AFM phase (a,b) and topographical (c,d; *z*-scale is 3 nm) images of nanofibrillar structures assembled from molecule **3** at 20 mN/m (a,b) and 0.2 mN/m (c,d). An example of a cross section across different nanofibers (see insert, 200 × 200 nm^2) collected with the carbon nanotube tip and used for true nanofiber diameter calculations (d).

by the fact that molecule **1** did not form well-defined nanostructures within the monolayer. Instead, uniform dense LB monolayers with the effective thickness of 3−4 nm were observed for molecules **1** transferred at the solid substrate at different surface pressures. Finally, the fractionation of the material was important for obtaining well-developed nanostructures. Although the amphiphilic molecules based on the other fractions of the core with lower molar weight were capable of forming partially ordered surface structures remotely resembling those discussed above, they were much less defined and stable.

To interpret these data and suggest an appropriate model of molecular packing within these nanofibers, we considered various possible molecular conformations of the amphiphilic hyperbranched molecules onto a hydrophilic surface including widely accepted edge-on and face-on packing of the flattened cores.[6,35] However, the comparison of corresponding molecular dimensions and the results of X-ray reflectivity studies of the molecule **3** at the air−water interface discussed below effectively excluded any symmetrical modes of molecular ordering.

In fact, X-ray reflectivity curves from the Langmuir monolayers of molecule **3** displayed well developed minima as can be observed in Figure 7. This reflectivity curve shape indicated the formation of a uniform dense monolayer with a nanometer-scale thickness at the air−water interface. The distribution of the electronic density along the surface normal calculated from the X-ray reflectivity data by using Fourier transformation and box model (see Supporting Information)[36−38] demonstrated that at the low surface pressure the alkyl tails with higher electron density were arranged at the water surface forming the topmost layer with about a 2 nm effective thickness (Figure 7). A broad transition zone indicated intensive clustering of molecules and the formation of the isolated surface structures which can be associated with nanofiber formation at the air−water interface.

Correspondingly, at the low surface pressure, the polyester cores formed the depleted, partially dehydrated sublayer at the air−water interface with a loose intermolecular packing (Figure 7). At higher surface pressure, in the condensed monolayer state, the alkyl tails predominantly orient themselves upward and the total effective monolayer thickness increased to 3.5 nm. This value is fairly close to the effective thickness of about 4 nm deducted from independent ellipsometric measurements of the monolayer transferred to the solid substrates at high surface pressure (see Suppporting Information). At this state, the cores became integrated in the region of alkyl tail packing.

In the condensed state, the terminal alkyl tails from the outer shell formed a poorly defined paracrystalline lattice with the hexagonal lateral packing as can be judged from the presence of a single intensive but relatively wide peak on the X-ray diffraction curves obtained directly from Langmuir monolayer

(35) Engelkamp, H.; Middelbeek, S.; Nolte, R. J. *Science* **1999**, *284*, 785.
(36) Vaknin, D. In *Methods of Materials Research*; Kaufmann, E. N., Abbaschian, R., Baines, P. A., Bocarsly, A. B., Chien, C. L., Doyle, B. L., Fultz, B., Leibowitz, L., Mason, T., Sanches, J. M., Eds.; John Wiley & Sons: New York, 2001.
(37) Weissbuch, I.; Leveiller, F.; Jacquemain, D.; Kjaer, K.; Als-Nielsen, J.; Leiserowitz. L. *J. Phys. Chem.* **1993**, *97*, 12858.
(38) Vaknin, D.; Kelley, M. S. *Biophys. J.* **2000**, *79*, 2616.

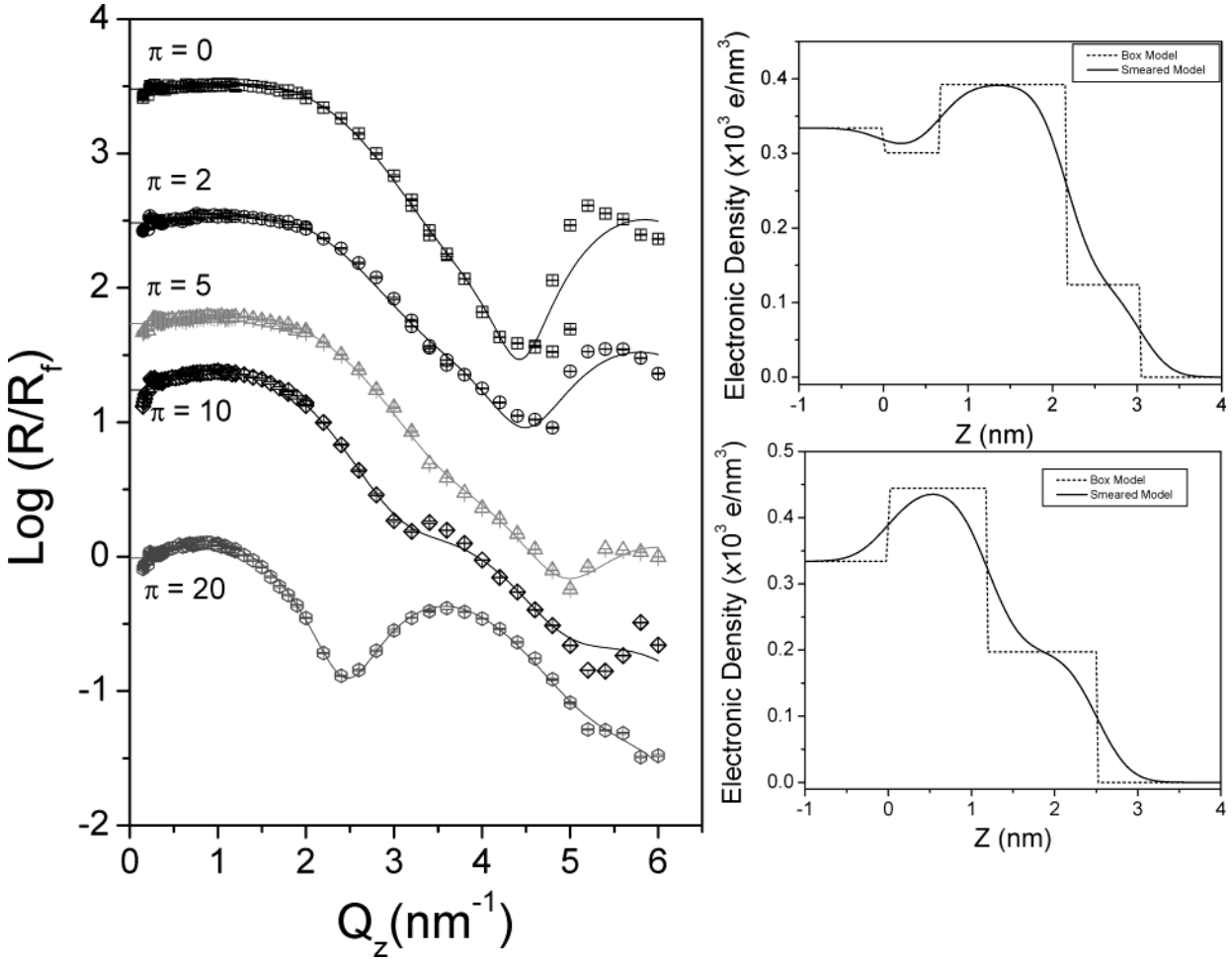

Figure 7. X-ray reflectivity data (relative intensity versus wavenumber) for molecule **3** at different surface pressures (in mN/m, left) and electronic density profiles at low (2 mN/m, top) and high (20 mN/m, bottom) surface pressures with sharp and diffuse interfaces (right).

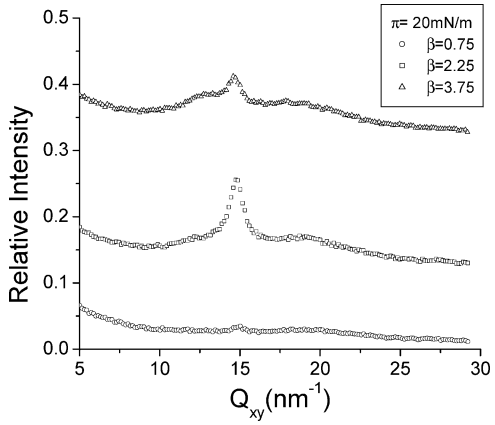

Figure 8. X-ray diffraction data for the monolayer from molecule **3** at three azimuthal angles. The appearance of a sharp peak at intermediate angle confirms tilted orientation of alkyl tails.

(Figure 8).[33] The lattice parameter of the corresponding unit cell of the alkyl tails was determined to be 0.492 nm, which is very close to the value usually detected for Langmuir monolayers from amphiphilic dendritic compounds with the outer alkyl shell when conventional hexagonal or orthorhombic unit cells of the alkyl tails were disturbed by the chemical attachment to a central branched core.[39,40] The alkyl tails of the compressed hyperbranched molecules were predominantly tilted with an average tilting angle of about 35°. The extension of the lateral ordering estimated from the corresponding correlation length did not exceed 5 nm that indicates very limited positional correlations in the packing of terminal alkyl tails not extending far beyond a single molecule.

Model of Molecular Packing. Therefore, the combined analysis of the AFM images and X-ray reflectivity data on the nanofiber dimensions, the Langmuir isotherm data of the molecular areas, the X-ray diffraction data on the tail orientation, along with the molecular dimensions from minimized molecular models allowed us to suggest an asymmetric model of the molecular packing for these nanofibers as presented in Figure 9.

In this model, the amphiphilic hyperbranched molecules adapt a highly asymmetric conformation, which is very different from the symmetrical extended conformation observed for undisturbed molecule and appropriate for face-on packing at the surface (Figure 9). The proposed model is a semispherical conformation in which the hydrophilic cores are squashed against the solid surface and the hydrophobic terminal branches are concentrated

(39) (a) Larson, K.; Vaknin, D.; Villavicencio, O.; McGrath, D.; Tsukruk, V. V. *J. Phys. Chem.* **2002**, *106*, 7246. (b) Larson, K.; Vaknin, D.; Villavicencio, O.; McGrath, D.; Tsukruk, V. V. *J. Phys. Chem.* **2002**, *106*, 11277. (c) Sidorenko, A.; Houphouet-Boigny, C.; Villavicencio, O.; McGrath, D. V.; Tsukruk, V. V. *Thin Solid Films* **2002**, *410*, 147. (d) Peleshanko, S.; Sidorenko, A.; Larson, K., Villavicencio, O.; Ornatska, M.; McGrath, D. V.; Tsukruk, V. V. *Thin Solid Films* **2002**, *406*, 233.

(40) Zhai, X.; Peleshanko, S.; Klimenko, N. S.; Genson, K. L.; Vortman, M. Y.; Shevchenko, V. V.; Vaknin, D.; Tsukruk, V. V. *Macromolecules* **2003**, *36*, 3101.

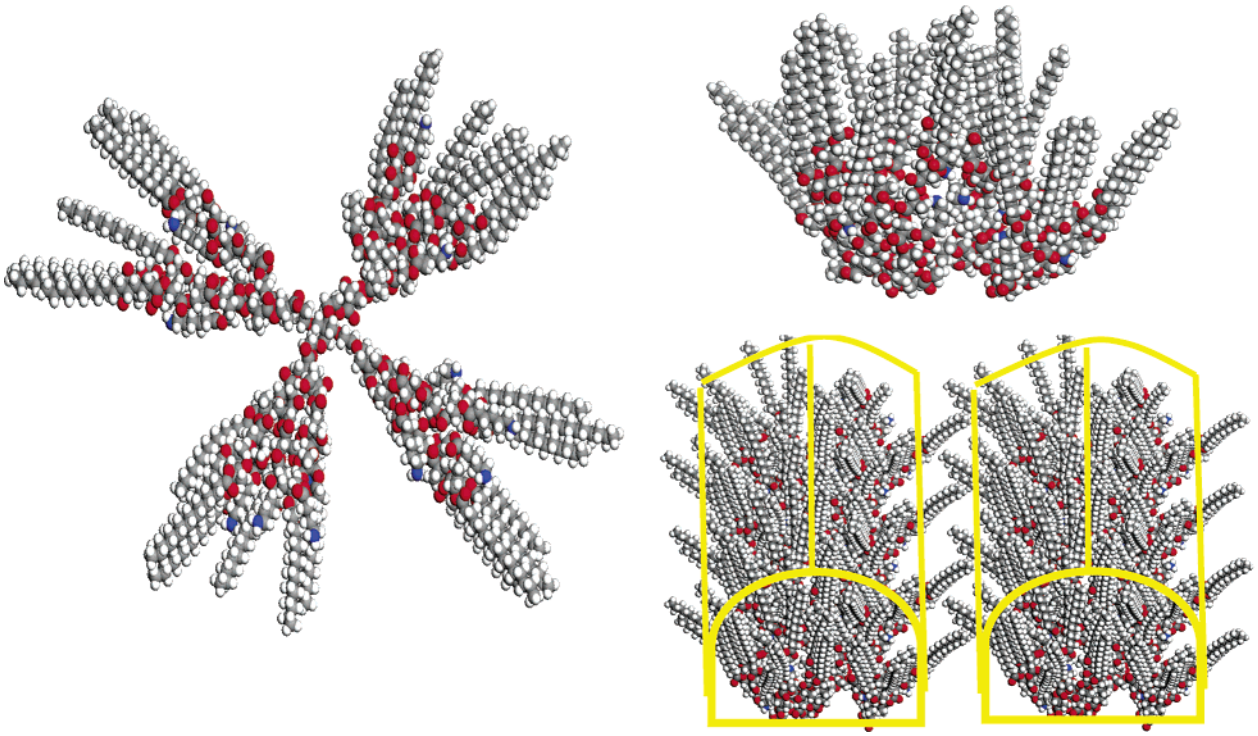

Figure 9. Molecular graphics of possible conformations and assemblies of amphiphilic hyperbranched molecule **3**: flat-on extended conformation (left, top view), compact asymmetric conformation (right, top, front view), and assembling in the semicylindrical, one-dimensional structures (right, bottom, top front view).

in the topmost layer (Figure 9). This conformation is similar to that speculated for regular amphiphilic dendrimers[6,20] and to that suggested for other amphiphilic hyperbranched molecules at hydrophilic surfaces.[40] However, it is also very different from the previous models which suggested a symmetrical, disklike shape of the flattened core in a face-on position. In the model proposed here, *the laterally compressed central core* must be suggested to allow for staking into one-dimensional structures (Figure 9). Both cores and shells should be slightly compressed in one direction to provide dense packing along the nanofiber axis.

The hydrophobic alkyl tails dominating the outer shell were oriented upward and tilted and covered most of the core, thus, making them included in the shell packing as was concluded from X-ray data. This conformation suggested an overall height of the molecules packed in nanofibers of 2.5−4 nm and the lateral dimensions of 4−8 nm depending upon the degree of alkyl tail orientation, packing density, and core conformation which correlate well with the dimensions obtained independently from different techniques. Dense stacking packing of the laterally compressed cores provided the way to assemble them in one-dimensional continuous rows resembling semicylindrical micelles. The calculated surface area per molecule for this arrangement was about 11 nm^2, which is close to Langmuir isotherm results on the onset of the formation of the condensed monolayer. Finally, this molecular packing should result in a modestly hydrophobic surface that is confirmed by contact angle measurement (within 60−80°). This conformation also maximizes favorable and strong interactions between amine terminal groups and the silanol surface groups which are critical for the nanofiber formation.[41]

Considering overall symmetrical chemical architecture of the modified molecules, their ability to form one-dimensional structures observed here is puzzling. Although further studies are required, we suggest that the one-dimensional molecular packing presented here for the explanation of the experimental data could be caused by the directional crystallization of alkyl tails oriented vertically in a central portion of the molecules with more distorted alkyl tails along the nanofiber edges preventing further crystallization in the lateral direction. In fact, molecules **3** can be crystallized in the bulk state with a melting temperature close to 35 °C.

It is also important that the packing structure proposed provided the best chance for the amine, hydroxyl, ester, and carboxyl groups of the cores and the inner shells of neighboring molecules to form a saturated network of hydrogen bonding and strong polar interactions without significant interference with the packed alkyl tails.[42] The critical role of these interactions has been supported by the fact that similar molecules (molecule **1**) without amine groups do not form nanofibrillar structures as was noted above despite their amphiphilic character. We believe that the presence of the amine groups strongly interacting with silanol groups of the silicon oxide surface layer of silicon wafers is critical in stabilization of these surface nanostructures. The mobility of these groups attached to the branches with flexible spacers can be an additional factor facilitating conformed intermolecular interactions. Molecules **1** contains only carboxyl and hydroxyl groups "built-in" the backbones which limits their mobility and flexibility and creates conditions for intramolecular hydrogen bonding. In fact, FTIR studies confirmed that despite the original core is rich in hydrogen bonding as indicated by a strong broad adsorption band in the range 3100−3900 cm^{-1},

(41) Tsukruk, V. V.; Bliznyuk, V. N. *Langmuir* **1998**, *14*, 446.

(42) Schneider, S. *Hydrogen Bonding*; Oxford University Press: New York, 1997.

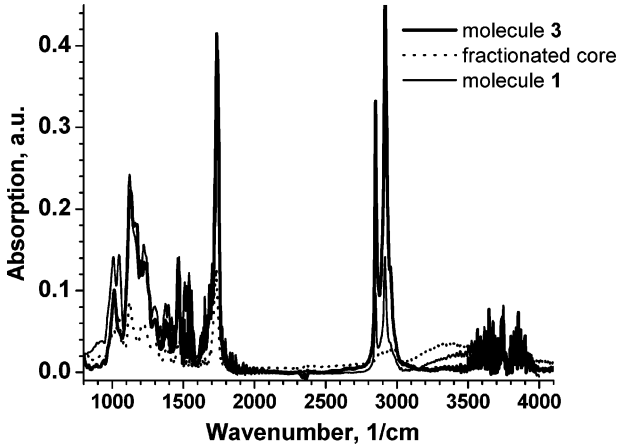

Figure 10. FTIR spectra for compounds studied.

molecule **3** shows a series of sharp adsorption peaks shifted to 3600−3800 cm^{-1} indicating amine-related vibrations with very little left of the original adsorption band (Figure 10). Meanwhile, molecules **1** still show a significant hydrogen bonding contribution within virtually the same spectral region (Figure 10).

We suggested that an initial spreading of amphiphilic hyperbranched molecules at the air−water interface in a "gas state" (isolated molecules at low surface pressure) combined with high molecular mobility was crucial for disbanding a strong association existing in solution[28] followed by one-dimensional supramolecular aggregation at the solid substrate. A critical role of the assembling conditions such as initial surface spreading was confirmed by the fact that such one-dimensional supramolecular structures were not formed when a physical adsorption or spin-casting from the solution was used as an alternative way to deposit molecules on the solid substrate. Additionally, the important roles of the chemical composition, the total molecular weight of the molecules, and polydispersity are clear from the fact that the lower molecular weight fraction did not form well-defined fibrillar structures and nonfractionated material did not show any of this type of surface behavior at all. We believe that in both cases the presence of the low molecular weight fraction with fewer alkyl tails in the shell and polar groups in the core disturbs the balance of intermolecular interactions along the fibrillar structures leading to the disruption of their uniformity.

Crystallization from Solution. The critical role of the alkyl tail crystallization was confirmed while conducting slow crystallization of this material (Figure 11). In fact, we observed that the crystallization of these hyperbranched molecules, if conducted under slow solvent evaporation conditions (gel crystallization), resulted in the formation of remarkably perfect and macroscopically long microfibrillar structures (Figure 11). These perfectly straight microfibers with the diameter from tens of a nanometer to hundreds of a micron and the length reaching several centimeters represent an example of very intriguing one-dimensional aggregation/crystallization of the same highly branched molecule but on a much larger spatial scale. These unique microfibers possessed a multishell internal microstructure and can be easily dissolved, remelted, and recrystallized.

Concluding Remarks

The formation of long, uniform nanofibers and nanoribbons with truly molecular lateral dimensions is a rare event observed

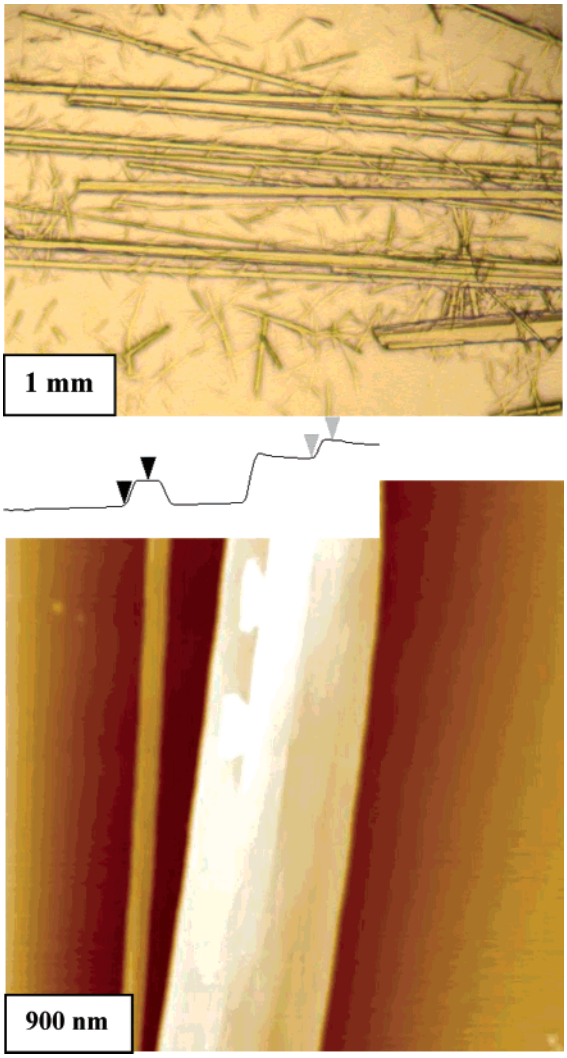

Figure 11. Optical micrograph (top) and AFM topographical image (bottom, 100 nm *z*-scale) of microfibers of molecule **3** crystallized from solution. For AFM image, insert shows the transversal cross section.

only for some organic and polymeric molecules.[12] We believe that cylindrical and semicylindrical micellar structures, closest to those reported here, were observed for low-molar mass ionic surfactants on solid surfaces.[43,44] A fine balance of weak intermolecular interactions was considered to be crucial for the formation of these fragile surface micellar structures. These metastable, semicylindrical micelles from conventional surfactants were easily disrupted by adsorption and drying conditions or AFM scanning with modest forces and did not form microscopically continuous fibers. Most of the AFM images confirming these surface structures were conducted directly in solvent with very low normal forces applied on very limited surface areas of several hundred nanometers. In contrast, the core−shell architecture of the amphiphilic hyperbranched molecules synthesized here shaped one-dimensional supramolecular nanofibrillar structures in a unique and very stable way. The multiple intermolecular hydrogen bonding and polar interactions between the flexible cores stabilized these nanofibers and made them *robust albeit flexible*. In fact, they were extremely stable during transfer, under high compression and

(43) Gaub, H. E.; Manne, S. *Science* **1995**, *270*, 1480.
(44) Ducker, W. A.; Wanless, E. J. *Langmuir* **1999**, *15*, 160.

dry conditions, were not disrupted by scanning with high forces, and were extending uninterrupted over many microns.

The very peculiar internal organization of these stable nanofibers with a hydrophilic inner core and hydrophobic shell makes them an intriguing candidate for the templating of inorganic wired nanostructures similarly to that already demonstrated for rigid molecules.[2,12] However, we believe that these flexible branched molecules can be much more versatile than complex molecules proposed earlier because their straightforward synthesis which could be easily adapted to produce significant quantities far exceeding minute amounts of regular amphiphilic dendrimers and complex shape-persistent molecules available.[45] Moreover, our findings question the current paradigm which calls for well-defined, shape-persistent, and rigid molecules with a precise placement of functionalized groups as the building blocks for one-dimensional supramolecular nanostructures. Indeed, we have found that the amplification of weak, directional interactions facilitated by the presence of multiple peripheral branches of even irregular, flexible molecules can lead to their efficient self-assembly into remarkably stable and uniform nano- and microfibrillar structures. Furthermore, this example demonstrates that one-dimensional supramolecular assembling can be achieved by using highly branched but irregular molecules without a tedious, multistep synthesis of the shape-persistent molecules.

Acknowledgment. This work is supported by the NSF-DMR-0308982 project, AFOSR F496200210205 grant, and DOE Advanced Photon Source, GUP-660 award. The authors thank Perstorp Polyols for materials donation, R. Gunawidjaja and J. Holzmueller for technical assistance, and D. Vaknin for help with X-ray reflectivity studies.

Supporting Information Available: Experimental routines for synthesis, fabrication, and characterization. This material is available free of charge via the Internet at http://pubs.acs.org.

JA0498944

(45) (a) Nguyen, C.; Hawker, C. J.; Miller, R. D.; Huang, E.; Hedrick, J. L.; Gauderon, R.; Hilborn, J. G. *Macromolecules* **2000**, *33*, 4281. (b) Sendijarevic, I.; McHugh, A. J.; Markoski, L. J.; Moore, J. S. *Macromolecules* **2001**, *34*, 8811.